

## MICROSTRUCTURAL AND MECHANICAL CHARACTERIZATION OF COMPOSITE ELECTROLESS NI-P-WC COATINGS ON DUCTILE IRON

---

**R. Valdez**

Centro de Ingeniería de Superficies y Acabados (CENISA). Facultad de Ingeniería. UNAM

**A. Bolarín**

Área de Ciencias de la Tierra y Materiales. Universidad Autónoma del Estado de Hidalgo

**F. Sánchez**

Área de Ciencias de la Tierra y Materiales. Universidad Autónoma del Estado de Hidalgo

**G. Agredo**

Departamento de Ingeniería Mecánica y Mecatrónica. Universidad Nacional de Colombia. Sede Bogotá

**R. González**

Centro de Ingeniería de Superficies y Acabados (CENISA). Facultad de Ingeniería. UNAM

**H. Waage**

Centro de Ingeniería de Superficies y Acabados (CENISA). Facultad de Ingeniería. UNAM

All content in this magazine is licensed under a Creative Commons Attribution License. Attribution-Non-Commercial-Non-Derivatives 4.0 International (CC BY-NC-ND 4.0).



**A. Coveló**

Centro de Ingeniería de Superficies y  
Acabados (CENISA). Facultad de Ingeniería.  
UNAM

**M. Hernández**

Centro de Ingeniería de Superficies y  
Acabados (CENISA). Facultad de Ingeniería.  
UNAM

**A. Barba**

Centro de Ingeniería de Superficies y  
Acabados (CENISA). Facultad de Ingeniería.  
UNAM

**Abstract:** This paper presents the results from the microstructural characterization of electroless nickel-plated pearlitic matrix ductile irons. Electroless Ni-P coatings have been obtained and composite electroless Ni-P and Ni-P-WC particles have been generated. The coatings achieved have been characterized by means of optical microscopy, scanning electron microscopy, EDS chemical microanalysis, X-ray diffraction, Vickers microhardness and wear resistance testing. The obtained results allow to distinguish that homogeneous coatings in thickness and with a good distribution of particles were achieved in the case of the Ni-P-WC coatings than in the Ni-P-SiC coating. Likewise, the structural characterization allowed to determine that the Ni-P coatings have an amorphous nature, and that the ceramic particles incorporated in the coatings allowed to improve the hardness (of the order of 100%) of the coatings.

**Keywords:** Microstructural characterization, ductile iron, Composite electroless nickel coatings.

## INTRODUCTION

Ductile irons are Fe-C alloys with carbon contents higher than steels (frequently between 3.0 and 3.5%), and presence of silicon in significant amounts (usually 2.5%). Their applications are wide in industries such as the automotive and the agricultural, to mention a few examples. Significant advances have been made with this type of materials recently; the application of heat treatments and the incorporation of carbide-forming elements have allowed to obtain materials such as the austempered ductile iron (ADI) and the carbide austempered ductile iron (CADI). These processes have substantially improved the mechanical properties of ductile irons. This way, ductile irons are suitable for a greater number of applications, even in competition with other ferrous and non-

ferrous alloys [Nofal et al, 2009; Keough et al, 2010]. Beside these characteristics, ductile irons have a slightly lower density ( $7.2 \text{ g/cm}^3$  is a typical value, although it depends on the grade of ductile iron) than steels ( $7.8 \text{ g/cm}^3$ ) and a melt point temperature also lower than that of steels, with which nodular cast irons are attractive as a potential alternative, often at a lower price, than other types of metallic materials for a variety of possible applications. Their wear resistance is quite acceptable; this property is associated with the presence of graphite in the form of nodules, which performs a lubricating action when this type of alloy comes into contact with the surface of other materials [Acosta et al, 2000; Wang et al, 2020]. However, there are aspects that should be improved to enhance their performance, such as their corrosion resistance in various environments.

Electroless nickel plating is a process in which an autocatalytic chemical reduction of nickel ions occurs in a solution, through the action of a reducing substance and without the use of an electric current. The most used reducing substance is sodium hypophosphite and the result is the deposition of Ni-P alloys, unlike what happens in the electrolytic process, (where pure nickel is deposited). The phosphorus content depends on the composition of the bath and, therefore, on the pH of the solution. This implies a structural modification [Gomes et al, 2019]. It is worth noting that the heat treatment applied to the electroless nickel coatings causes changes in their microstructure, especially if the coatings have a phosphorus content greater than 9.5%, and that the modifications that include the formation of crystalline Ni and  $\text{Ni}_3\text{P}$  significantly decrease the corrosion resistance of the deposits. [Palaniappa et al, 2007; Keong et al, 2003, Keong et al, 2002]. In relation to the behavior of ductile irons under corrosion conditions, studies such as

[Lelito et al, 2009, Arenas et al, 2014] report how it can be considered that their corrosion resistance is low in some media. This behavior is considered to be associated with the formation of unprotective corrosion products and with the generation of galvanic cells associated with the presence of graphite. Thus, it is relevant to improve this performance, given the growing use of ductile irons in technological applications. The proposed ways to improve the resistance to corrosion of the material are: the modification of the chemical composition, the application of heat treatments and the use of various types of surface treatments. In fact, the effect of the silicon content of the alloy was evaluated and a slight improvement in corrosion resistance was found without substantial change in its mechanical properties [Arenas et al, 2014], which was proposed as an alternative to study in future works. The application of austempering processes and the addition of carbide-forming elements have given rise to the formation of ADI and CADI, as indicated above. In general, it is reported that the austempered ductile iron presents better resistance to corrosion in NaCl solution than the ductile iron without this treatment. In this sense, it is reported that higher austempering temperatures decrease corrosion resistance, and that, at these temperatures, longer treatment times decrease corrosion speed and the opposite occurs at lower austempering temperatures, that increase their corrosion rate [Mahadik et al, 2016; Mahadik et al, 2017]. Regarding the application of surface treatments, in [Ordoñez et al, 2012] the austempering treatment is combined with a boronizing of a ductile iron and a significant increment in its microhardness is reported, which could help improve its behavior under wear conditions. Other treatments that have been applied are related to the use of laser radiation [Schaaf, 2002]; these treatments

have allowed to achieve substantial increases in the microhardness of the surface by controlling the cooling rates of the processes of boronizing. Regarding the application of electroless nickel plating processes on ductile irons, a variety of works have made various contributions to understand how does the process occur in these alloys and what modifications does it produce in their properties. For example, [Forestier et al. 2018] point out how the presence of graphite in spheres can complicate the electroless nickel plating process and propose a model for the formation of the deposit and its growth. On the other hand, in [Hsu et al, 2005; Hsu et al, 2009; Biswas et al 2018], the use of electroless nickel deposits is proposed as part of duplex coatings on ductile irons. The combination of these type of deposits with other other surface technologies can improve the adherence, as well as the resistance to corrosion and wear of this type of ferrous alloys. It is worth mentioning an additional advantage, which is that electroless nickel plating (given the temperature at which the process is carried out) does not cause changes in the mechanical properties of ductile irons or those of austempered ductile iron. Another field that has been extensively explored is the addition of hard particles (usually ceramics) to electroless nickel plating baths to achieve what are known as composite electroless nickel coatings [Sudagar et al, 2013; Zhang et al, 2019; Sahoo et al-2011], finding that it usually increases the microhardness, as well as the wear resistance of the deposits. There are many particles that have been added, among the most common SiC, Al<sub>2</sub>O<sub>3</sub>, WC, TiO<sub>2</sub>, B<sub>4</sub>C, Si<sub>3</sub>N<sub>4</sub> and diamond, which, in several cases, have recently been incorporated into the process, using nanometric-sized particles. A variant in this regard is the addition of PTFE (Teflon) particles (for their lubricity qualities) with which relevant results have also been

achieved. As for composite electroless nickel platings on ductile iron and ADI, they are still rare.

The research potential is not over and the effects of this type of process on the properties of these ferrous alloys remain to be studied. In this work electroless nickel coatings with and without the addition of WC particles are deposited on a ductile iron and a study of the morphology, mechanical and microstructural characteristics of the coatings achieved is carried out in order to find the particularities associated with this type of coating.

## MATERIALS AND METHODS

The ductile iron sample was provided by the Department of Metallurgical Engineering of the Faculty of Chemistry of the UNAM. From the received material, 30 specimens of 2.5 cm length x 1.5 cm width were made by turning. Subsequently, they were subjected to a cleaning process with alkaline and acid stages and an ultrasonic cleaning in alcohol. The pieces were electroless nickel-plated using a bath as the one reported in [Barba, A.,1997], at 86°C, using times of 3 and 5 hours and with the addition of 0.003 M WC (Sigma-Aldrich 99.8%, Dm,50<12 μm). Figure 1 shows the arrangement of the equipment used for the electroless nickel plating of the samples.

The deposits obtained with the electroless nickel plating were prepared for metallographic observation using 200 to 1000 grit sandpaper and then polished with 0.5 and 0.03 μm alumina, carrying out an attack with 2% nital. The coated pieces were further characterized by scanning electron microscopy, using a JEOL 5900 LV electron microscope and a Philips XL20 microscope, each coupled to an EDS microprobe to determine the semi-quantitative composition of the coatings. Likewise, the microhardness of the coatings was determined by means of a Matsuzawa Model MHT2 microhardness

tester using a 100 g<sub>F</sub> load for 10 seconds in various areas of the coatings, carrying out at least 10 measurements of each pieces with and without coating, with and without added WC particles. The structure of the coatings was evaluated employing X-ray diffraction at room temperature of 25 °C, a range between 15 and 90 ° was established, a time per step of 30 s, for a total scanning time of 7 min.

The evaluation of the tribological behavior was carried out by means of a pin on disc type test, in a wear test machine Model Cignus, manufactured by Swansea Tribology Centre. The specimens were manufactured with the geometry shown in Figure 2.

The contact area was 0.31 cm<sup>2</sup>, without lubrication, a distance of 1000 m, at a speed of 150 rpm and with a load of 1 Kg<sub>F</sub>. The wear coefficient was obtained using the following equation:

$$K = \frac{VH}{ws}$$

K: Wear coefficient

V: Volume of wear [mm<sup>3</sup>]

H: Hardness HB

w: Axial test load [kg<sub>F</sub>]

s: Sliding distance [mm]

## RESULTS AND DISCUSSION

Figure 3, obtained by scanning electron microscopy with secondary electrons, shows the microstructure of the ductile iron used as substrate, in which the presence of the pearlite and ferrite phases can be clearly distinguished, as well as a graphite nodules phase. This morphology is typically known as a “bull’s eye”. It should be noted that the predominant phase is perlite. To complete this observation, a chemical analysis of the nodular cast iron was carried out by the Faculty of Chemistry of the UNAM by means of atomic emission spectroscopy, these results are presented in Table 1.

Figure 4 presents an image from optical

microscopy of one of the electroless nickel coatings. The homogeneity of the deposit and the presence of each of the phases (pearlite, ferrite and graphite nodules) are highlighted.

Figure 5 shows a scanning electron microscopy image, with secondary electrons, of an electroless nickel coating on ductile iron. It can be seen that the coating is uniform in thickness and well adhered. The presence of graphite nodules is also highlighted.

Figure 6 presents the result of the EDS microanalysis for the coating, showing the presence of mostly Ni and P peaks, the presence of elements such as Fe and C, to a lesser extent, is due to the contributions of the elements that make up the substrate.

Figure 7 shows the diffractogram of an electroless nickel plating layer obtained on the ductile iron, without the addition of particles. The amorphous nature of the coating was observed with a peak centered at  $2\Theta=44.7^\circ$  according to the ICSD 01-070-0989 reference pattern. The crystallinity of the coating was calculated as the ratio of the area under the curve, obtaining 80% amorphousness of the deposit. This amorphous character is preserved in the coatings with the addition of WC particles, in accordance with what was reported in [Barba A, 1997, Al-Ageeli et al, 2014, Hamid et al, 2007)].

The presence of W and C, in addition to Ni and P can be observed in the EDS spectrum of Figure 8, with which it is possible to corroborate that it is very probable that the tungsten carbide particles have been co-deposited, which can be verified in microscopic observations below.

Figure 9, which presents scanning electron microscopy images, shows the morphology, in top view, of the electroless nickel coating without the addition of particles on the nodular cast iron, after a 3-hour process. The Ni-P coating presents a predominance of spherical geometry, typical of this type of

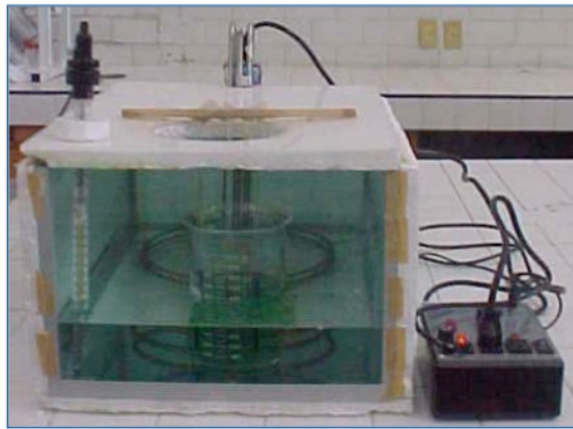


Figure 1. Equipment used to carry out electroless nickel plating of ductile iron parts.

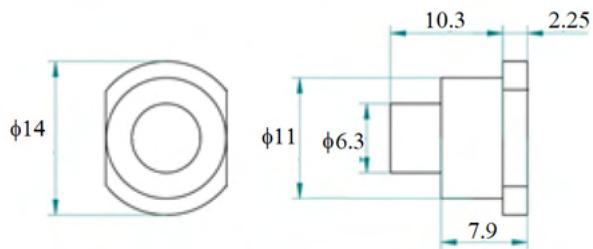


Figure 2. Geometry of the specimens used for the pin on disc type wear test. Units in mm.

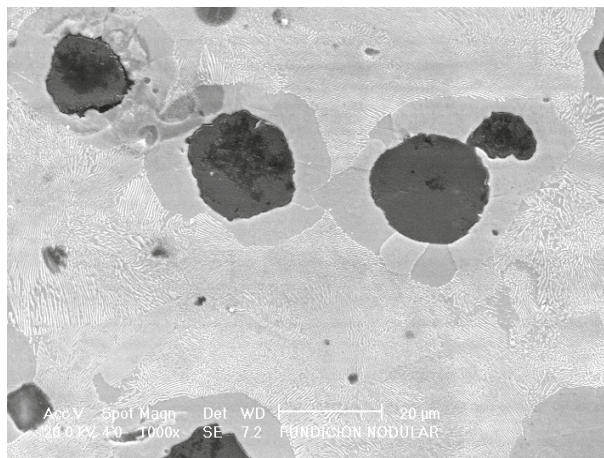


Figure 3. Scanning electron microscopy image of the perlitic ductile iron used as a substrate for electroless nickel plating, 1000X-SE.

%Fe	% C	% Si	% Mn	% P
92.7	3.606	2.505	0.521	0.017

Table 1. Elemental composition of the study material. Weight percentage.

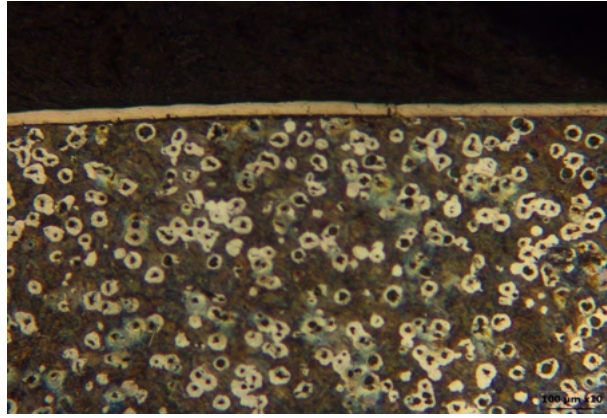


Figure 4. Optical microscopy image of the electroless nickel deposit on ductile iron. The presence of ferrite, pearlite and graphite nodules phases stands out. In addition, the homogeneity of the deposit. 10X - OM.

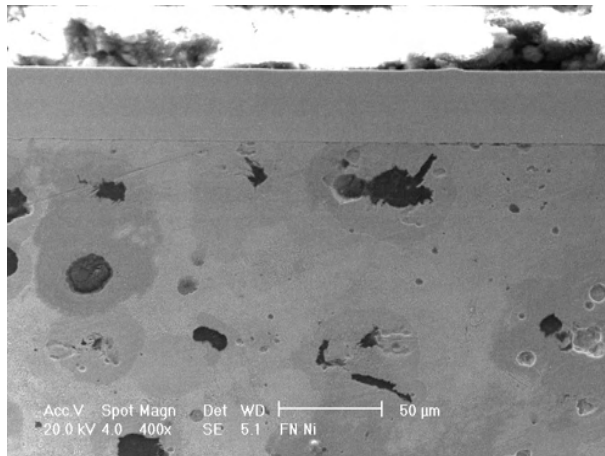


Figure 5. Scanning electron microscopy image of an electroless nickel deposit on a ductile iron sample. The thickness is little less than 50μm. 400X - SEM. SE

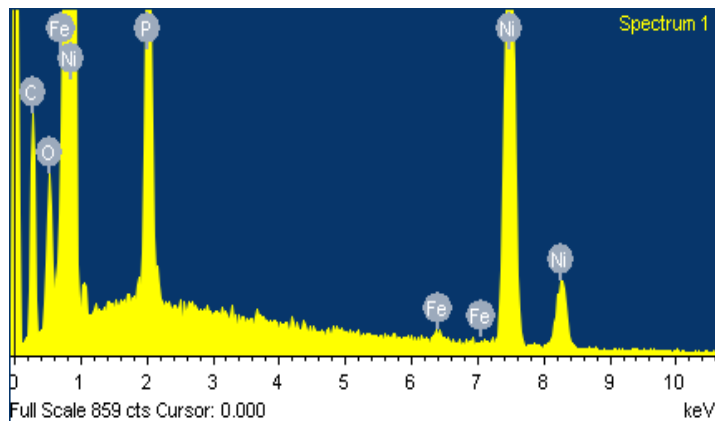


Figure 6. EDS spectrum of the electroless nickel coating on ductile iron, in which the presence of Ni is distinguished and P from the lining and Fe, C from ductile iron. The O may come from some oxide that may have formed on the surface prior to the process.

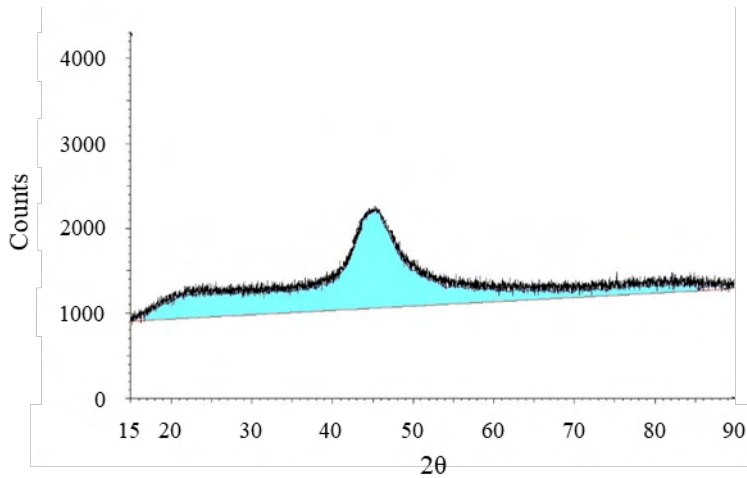


Figure 7. Diffractogram of the electroless nickel deposit on ductile iron. The amorphous condition of the coating stands out with the peak presented at an angle close to 45°.

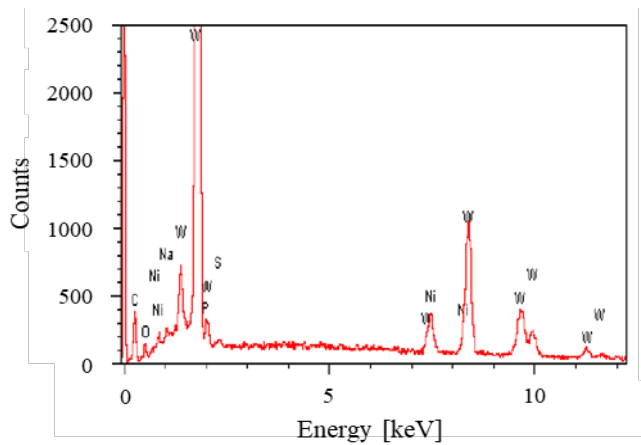


Figure 8. EDS spectrum of the composite electroless Ni-P-WC coating on a ductile iron sample, in which the presence of Ni and P of the coating and W and C of the added particles are distinguished.

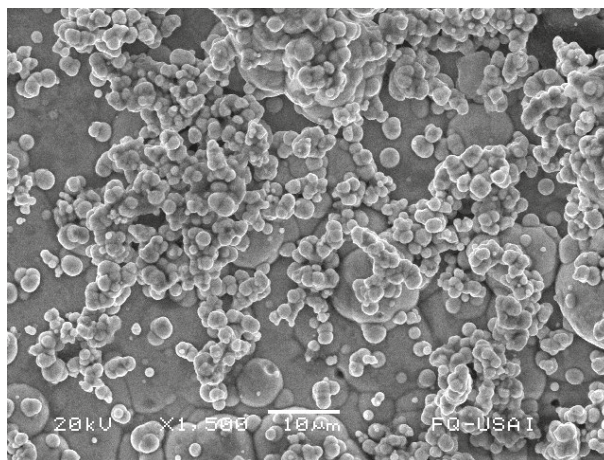


Figure 9. Scanning electron microscopy image of an electroless nickel deposit on a ductile iron sample, after 3 hours of processing. The spherical geometry of the layer stands out and the fact that, apparently, in some areas the coating is not observed. 1500X-SE.

coating [Barba A, 1997, Al-ARGEELI et al, 2014; Hamid et al, 2007]. It should also be noted that after 3 hours (layer thickness was about 10  $\mu\text{m}$ ) it appeared that some sections of the substrate were not coated.

In the scanning electron microscopy image shown in Figure 10, which corresponds to an electroless nickel coating without the addition of particles on a ductile iron sample, obtained after 5 hours of processing, a coating that has fully covered the surface is observed more compact, with a morphology similar to the one presented in Figure 9. It should be noted that the thickness was approximately 19  $\mu\text{m}$ . It should be reiterated that both images have been generated with the same level of magnification (1500X) and with the use of secondary electrons.

Figure 11 corresponds to an electroless Ni-P-WC deposit, obtained after 3 hours of processing. The approximately 17  $\mu\text{m}$  thick coating managed to cover the substrate, although the morphology has changed. It can be interpreted that the WC particles, which have agglomerated, due to their small size (<12  $\mu\text{m}$ ), have been adequately embedded in the original Ni-P layer, in agreement with what was reported in [Hamid et al, 2007].

Figure 12, from the observation of a composite electroless Ni-P-WC coating, after 5 hours of processing and with an approximate thickness of 40  $\mu\text{m}$ . The deposit shows conglomerates of WC particles and some areas where probably the WC particles could not be properly embedded in the Ni-P matrix, because it is complicated with continue to keep the particles within the solution given the high density of WC (15.63  $\text{g}/\text{cm}^3$ ) and the fact that the agitation conditions were probably not sufficient to achieve that purpose [Hamid et al, 2007, Prieto et al, 2005].

Figure 13 allow to observe the morphology of the isolated particles of WC. It is possible to relate these electron microscopy images to

those observed for Ni-P-WC.

When figures 11, 12 and 13 are compared, a similar morphology of the particles is perceived, if anything, as the number of increases in figure 12 is greater, the morphology and geometry of the WC particles themselves are more clearly distinguished.

Table 2 shows the microhardness values of ductile iron without coatings and of the ductile iron samples themselves with electroless Ni-P and Ni-P-WC coatings, after 5 hours of processing. Initially, it can be stated that the microhardness increases in an electroless Ni-P deposits, a little more than 100 Vickers units, with respect to the original of the ductile iron. In the case of the particles added to the composite electroless nickel coating, the increase achieved by adding them is evident in the case of the addition of WC particles, in which values close to 1000 Vickers are achieved.

In the case of the NiP coating, it improves by 5.8 times the wear coefficient and the NiP-WC coating by 4.6 times compared to the uncoated substrate.

In the case of electroless nickel plating, it can be seen that the composite coatings show very similar favorable results in terms of reducing the wear of ductile iron; the NiP coating slightly outperforms with a wear coefficient of 1.44E-05. This may be due to the fact that the NiP coating layer is more homogeneous, which could suggest for the composite coating with WC, that despite having hardness values of up to 958HV, the tungsten carbides in the added proportion do not seem to favor the performance of the coating (probably because the particles were not perfectly embedded and adhered), and could lead to a 2 and even 3-body wear mechanism due to the generation of loose abrasive particles between the coating and the moving disk, contributing to a greater loss of mass of the coating, but it will be necessary and convenient to carry out

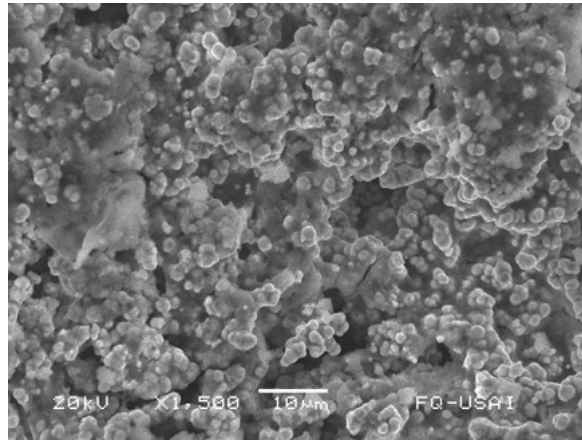


Figure 10. Scanning electron microscopy image of a nickel chemical deposit on a ductile iron sample, after 5 hours of processing. The predominantly spherical geometry of the layer stands out. The coating is more compact and covers practically the entire surface of the substrate. 1500X-SE.

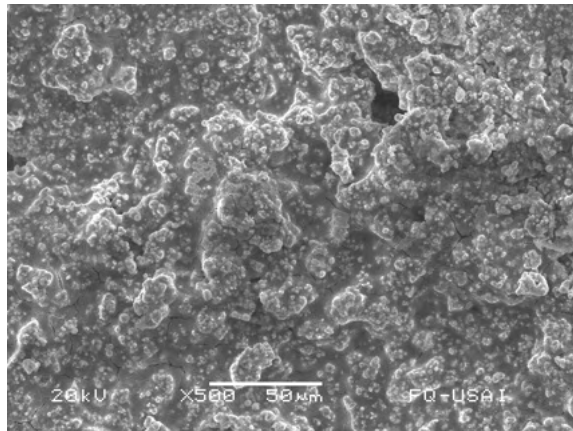


Figure 11. Scanning electron microscopy image of a composite electroless nickel with the addition of WC particles, on a ductile iron sample, after 3 hours of processing. The morphology has another aspect and it is perceived as compact, possibly because the WC particles could be properly embedded in the Ni-P matrix layer. 500X-SE.

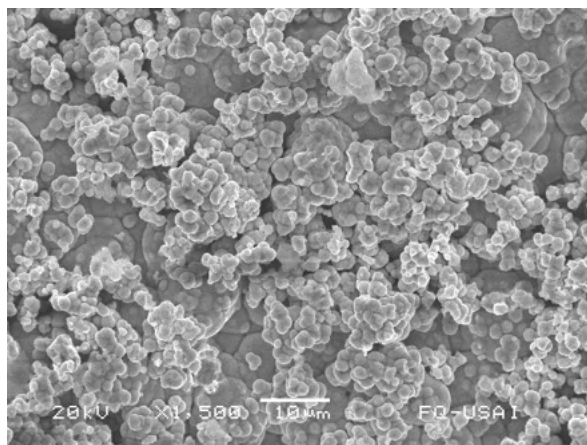


Figure 12. Scanning electron microscopy image of a composite electroless Ni-P-WC on a ductile iron sample, after 5 hours of processing. Some possibly uncoated areas are glimpsed. 1500X-SE.

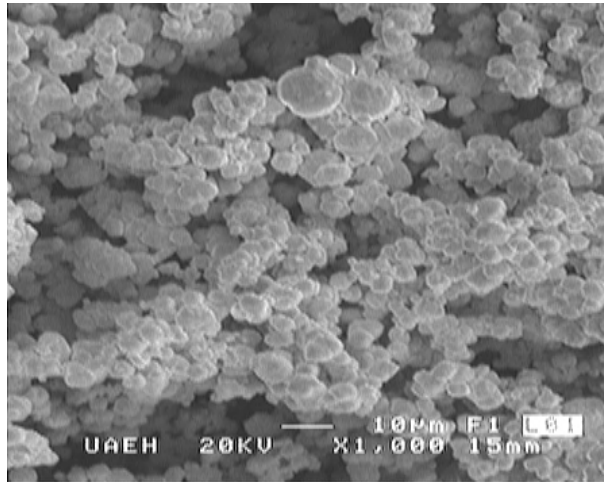


Figure 13. Scanning electron microscopy image of the WC particles, in which the condition of a geometry tending to be spherical and the formation of agglomerates of the particles themselves can be highlighted. 1000X-SE.

	Ductile Iron	Ni-P 5h	Ni-P-WC 5h
Microhardness HV	390.25	502.55	958.3

Table 2. Microhardness of electroless Ni-P and Ni-P-WC coatings.

Material	Wear Volume [cm <sup>3</sup> ]	Wear Coefficient
NiP	0.000128	1.44E-5
NiP-WC	0.000252	1.83E-5
Ductile iron	0.000850	8.35E-5

Table 3 – Wear coefficient results

more tests to corroborate it.

The performance of the generated coatings offers advantages for anti-wear applications with respect to bare substrates, however, for the case in which WC particles are added, low cohesion zones are generated, and surrounding porosity that promote the detachment of abrasive particles that accentuate the loss of material and do not contribute in the amounts added to improve its tribological performance with a tendency to accelerate wear. In any case, it will be necessary to look for mechanisms to improve the adherence of WC particles.

## CONCLUSIONS

1.- A microstructural study of electroless Ni-P and Ni-P-WC coatings has been carried out on a ductile iron sample. The generated Ni-P coatings, without particles, were uniform in thickness, well adhered and amorphous in nature, which was not modified when WC particles were added to the bath.

2.- In the case of composite electroless

Ni-P-WC deposits, the WC particles tend to agglomerate, due to their size (smaller than 12  $\mu\text{m}$ ) and, associated with this, for the times and conditions in which coatings were obtained, it was very difficult to achieve a deposit with uniform and homogeneous distribution of the particles.

3.- Regarding microhardness, the 5 hours process with added WC particles allowed to double its value.

## ACKNOWLEDGEMENTS

The authors of the Centro de Ingeniería de Superficies y Acabados (CENISA) of the Facultad de Ingeniería of the UNAM, thank the Dirección General de Asuntos del Personal Académico (DGAPA) of the UNAM, for the support provided through the PAPIIT Projects IT101221 “Desarrollo de Tecnologías Alternativas de Modificación de Superficies para la Mejora de Materiales de Potencial Industrial”.

## REFERENCES

- Acosta M.; Martínez M. López J. 2000. El tratamiento de los Hierros nodulares en el Mejoramiento de los materiales en la industria automotriz. Un Caso Práctico. Publicación Técnica No. 148. Secretaría de Comunicaciones y Transportes. Instituto Mexicano del Transporte. 1-69.
- Al-Aqeeli N, Saheb N., Laoui T. Mohammad K. 2014. The Synthesis of Nanostructured WC-Based Hardmetals Using Mechanical Alloying and Their Direct Consolidation. *Journal of Nanomaterials*, (2014), Article ID 640750, 16 pages.
- Arenas M, Niklas A, Conde A, Mendez S., Sertucha J., Damborenea J.. 2014. Comportamiento frente a la corrosión de fundiciones con grafito laminar y esférico parcialmente modificadas con silicio en NaCl 0,03 M. *Revista de Metalurgia* 50(4), e032. ISSN-I: 0034-8570.
- Barba A. 1997. Obtención y Caracterización de Recubrimientos Químicos Compuestos Ni-P-X ( $\text{Al}_2\text{O}_3$ , SiC) sobre Al. Tesis Doctoral. Universidad de Barcelona. 1997. Director: Pedro Molera Solá.
- Biswas N., Kumar R, Majumdar G., Brabazon D. 2018. Review of duplex electroless coatings and their properties, *Advances in Materials and Processing Technologies*. <https://doi.org/10.1080/2374068X.2018.1457298>.
- Forestier I, Berthomé G. Wouters Y. 2018. Study of Electroless Nickel Coatings on EN-GJS-500-7 Spheroidal Graphite Cast Iron. *Coatings*, 8, 239.
- Gomes N, González-Estrada O., Pertuz A. 2019. Electroless Nickel Phosphorous: una visión global, *Rev. UIS Ing.*, vol. 18, 4, 173- 192.

- Hamid Z, El Badry S, Aal A.** 2007. Electroless deposition and characterization of Ni–P–WC composite alloys. *Surface & Coatings Technology* 201. 5948–5953.
- Hsu C, Chen K, Lee C, Lu K.** 2009. Effects of low-temperature duplex coatings on corrosion behavior of austempered ductile iron. *Surface & Coatings Technology* 204 997–1001.
- Hsu C, Lu J, Tsai R.** 2005. Effects of low-temperature coating process on mechanical behaviors of ADI. *Materials Science and Engineering A* 398. 282–290.
- Keough J.** 2010. Austempered Ductile Iron (ADI) - A Green Alternative. Applied Process Inc. internal research. p. 1-8.
- Keong, K. G. Sha W., Malinov S.** 2002. Crystallisation kinetics and phase transformation behaviour of electroless nickel-phosphorus deposits with high phosphorus content. *Journal of Alloys and Compounds* 334. 192–199.
- Keong K.G.; Sha W., Malinov S.** 2003. Hardness evolution of electroless nickel–phosphorus deposits with thermal processing. *Surface and Coatings Technology* 168. 263–274.
- Krawiec H., Lelito J., Tyrała E., Banaś J.** 2009. Relationships between microstructure and pitting corrosion of ADI in sodium chloride solution. *J Solid State Electrochem.* 13:935–942. DOI 10.1007/s10008-008-0636-x.
- Mahadik S.P., Harne M.S. Patil S.A.** 2016. Study on Effect of Austempering Temperature and Time on the Corrosion Resistance of Carbide Austempered Ductile iron (CADI) Material. *IJSRD - International Journal for Scientific Research & Development* 4, 10, ISSN (online): 2321-0613. p. 401-406.
- Mahadik, S.P, Harne, M.S, Raka V.** 2017. Study on the effect of austempering temperature and time on the corrosion resistance of carbide austempering ductile iron (CADI) Material. *Journal of Advances in Science and Technology.* 13, 1 (2017). p. 234-240
- Nofal A.; Jekova L.** 2009. Novel processing techniques and applications of austempered ductile iron. (review). *Journal of the University of Chemical Technology and Metallurgy*, 44, 3, 213-228.
- Ordoñez U. Parada S. Diaz C., Barba A., Valdéz R., Hernández M.A, Covelo A.** 2012. Austenitización y Borurado Simultáneo de un hierro nodular austemperizado. *Memorias del XIX Congreso Internacional Anual de la Sociedad Mexicana de Ingeniería Mecánica.* 625-632. ISBN -978-607-95309-9-0.
- Palaniappa M., Seshadri S.** 2007. Structural and phase transformation behaviour of electroless Ni–P and Ni–W–P deposits. *Materials Science and Engineering A* 460–461. 638–644.
- Prieto F., Bolarín A., Sánchez F. Méndez A.** 2005. Efecto del sistema de agitación sobre la codepositación de alúmina químico compuesto. *Superficies y Vacío* 18(1).38-46.
- Sahoo P., Das S. K.** 2011. Tribology of electroless nickel coatings – A review. *Materials and Design* 32, 1760–1775.
- Schaaf P.** 2002 Laser nitriding of Metals. *Progress in Materials Science.* 47, 1-161.
- Sudagar J, Lian J., Sha W.** 2013. Electroless nickel, alloy, composite and nano coatings – A critical review. *Journal of Alloys and Compounds* 571. 183–204.
- Wang B. Barber B. Qiu F, Zou Q., Yang H.** 2020. A review: phase transformation and wear mechanisms of single-step and dual-step austempered ductile irons. *J. Mater. Res. Technol.* 9, (1). 1054-1069.
- Zhanga W, Caoa D, Qiaoa Y., Hea Z., Wanga Y., Lib X, Gao W.** 2019. Microstructure and Properties of Duplex Ni-P-TiO<sub>2</sub>/Ni-P Nanocomposite Coatings. *Materials Research.*; 22(suppl. 2): e20180748.